Transfer of pathogenic and nonpathogenic cytosolic proteins between spinal cord motor neurons in vivo in chimeric mice

Eleanor V. Thomas[a], Wayne A. Fenton[b], James McGrath[b,c], and Arthur L. Horwich[b,d,1]

[a]Interdepartmental Program in Neuroscience, Yale University School of Medicine, New Haven, CT 06510; [b]Department of Genetics, Yale University School of Medicine, New Haven, CT 06510; [c]Department of Comparative Medicine, Yale University School of Medicine, New Haven, CT 06510; and [d]Howard Hughes Medical Institute, Yale University School of Medicine, New Haven, CT 06510

Recent studies have reported spread of pathogenic proteins in the mammalian nervous system, but whether nonpathogenic ones spread is unknown. We initially investigated whether spread of a mutant amyotrophic lateral sclerosis-associated cytosolic superoxide dismutase 1 (SOD1) protein between motor neurons could be detected in intact chimeric mice. Eight-cell embryos from G85R SOD1YFP and G85R SOD1CFP mice were aggregated, and spinal cords of adult chimeric progeny were examined for motor neurons with cytosolic double fluorescence. By 3 mo of age, we observed extensive double fluorescence, including in amyotrophic lateral sclerosis-affected cranial nerve motor nuclei but not in the relatively spared extraocular nuclei. Chimeras of nonpathogenic wtSOD1YFP and G85R SOD1CFP also exhibited double fluorescence. In a third chimera, mitochondrial mCherry did not transfer to G85R SOD1YFP motor neurons, suggesting that neither RNA nor organelles transfer, but mito-mCherry neurons received G85R SOD1YFP. In a chimera of ChAT promoter-EGFP and mito-mCherry, EGFP efficiently transferred to mito-mCherry^{+} cells. Thus, nonpathogenic cytosolic proteins appear capable of transfer. During study of both the SOD1FP and EGFP chimeras, we observed fluorescence also in small cells neighboring the motor neurons, identified as mature gray matter oligodendrocytes. Double fluorescence in the G85R SOD1FP chimera and observation of the temporal development of fluorescence first in motor neurons and then in these oligodendrocytes suggest that they may be mediators of transfer of cytosolic proteins between motor neurons.

ALS | oligodendrocytes | cranial nerves | aggregates | SOD1

The spread of misfolded, pathogenic protein between cells in the mammalian nervous system has become evident in recent years from study of a number of neurodegenerative diseases, including spongiform encephalopathies, Parkinson's disease, and Alzheimer's disease (see refs. 1 and 2, for review). In particular, geographic movement of misfolded protein species characteristic of these diseases has been observed and associated with extension of cellular pathology and with clinical onset or progression (3–7). Beneath these observations, however, lies the question of whether nonpathogenic proteins might also be capable of transfer, for example, between neurons. Here, in the context of addressing "spread" of a mutant amyotrophic lateral sclerosis (ALS)-producing superoxide dismutase 1 (SOD1) protein in a mouse system, we have accreted evidence that normal nonpathogenic cytosolic proteins can also transfer between motor neurons.

In studies of patients with ALS, there has been the suggestion that the temporal progression of motor symptoms from an initial extremity to eventually affect the others could relate to a spread of pathogenesis within the motor system (8). Within the ~10% of ALS cases that are heritable, a portion (~20%) involve mutation, misfolding, and aggregation of the abundant cytosolic protein SOD1 (9–12). This state has been modeled in mice transgenic for various mutant human SOD1 transgenes (13, 14). Recent studies, both in cells in culture (15, 16) and in mice injected with homogenate from end-stage paralyzed mice (17–19), have suggested that

mutant SOD1 can spread between motor neurons. In an effort to study whether mutant misfolded SOD1 can spread in vivo in intact mice in the absence of injection, we produced chimeric mice from two mutant human SOD1 transgenic ALS strains, one bearing mutant (G85R) SOD1 fused to YFP (20) and the other fused to CFP. After aggregating eight-cell embryos of the two different strains, chimeric offspring were studied to ascertain whether the distinct G85R SOD1YFP and G85R SOD1CFP fluorescent proteins could at any point be observed in the same spinal cord motor neurons. The positive results led us to form additional chimeras with wild-type versions of SOD1 and with other nonpathogenic proteins. Evidence of transfer of cytosolic proteins between motor neurons is presented, as well as identification of a possible cellular intermediate of such transfer, mature oligodendrocytes.

Results

Production of Chimeric Mice from ALS-Associated G85R SOD1YFP and G85R SOD1CFP Transgenic Strains. To investigate whether mutant SOD1 transfers between motor neurons in the spinal cord in vivo, we generated chimeric mice by mixing embryos at the eight-cell stage from two transgenic strains that develop ALS from expression of mutant human SOD1, one expressing G85R SOD1YFP and the other expressing G85R SOD1CFP (Fig. 1A). Motor neurons in the chimeras should exhibit either YFP or CFP fluorescence if no transfer occurs between them, and they should exhibit both YFP and CFP fluorescence if transfer is occurring (Fig. 1A). The G85R SOD1YFP strain, produced and characterized in our laboratory (20), expresses a G85R SOD1YFP fusion protein from a transgenic human genomic clone that includes the human SOD1 promoter
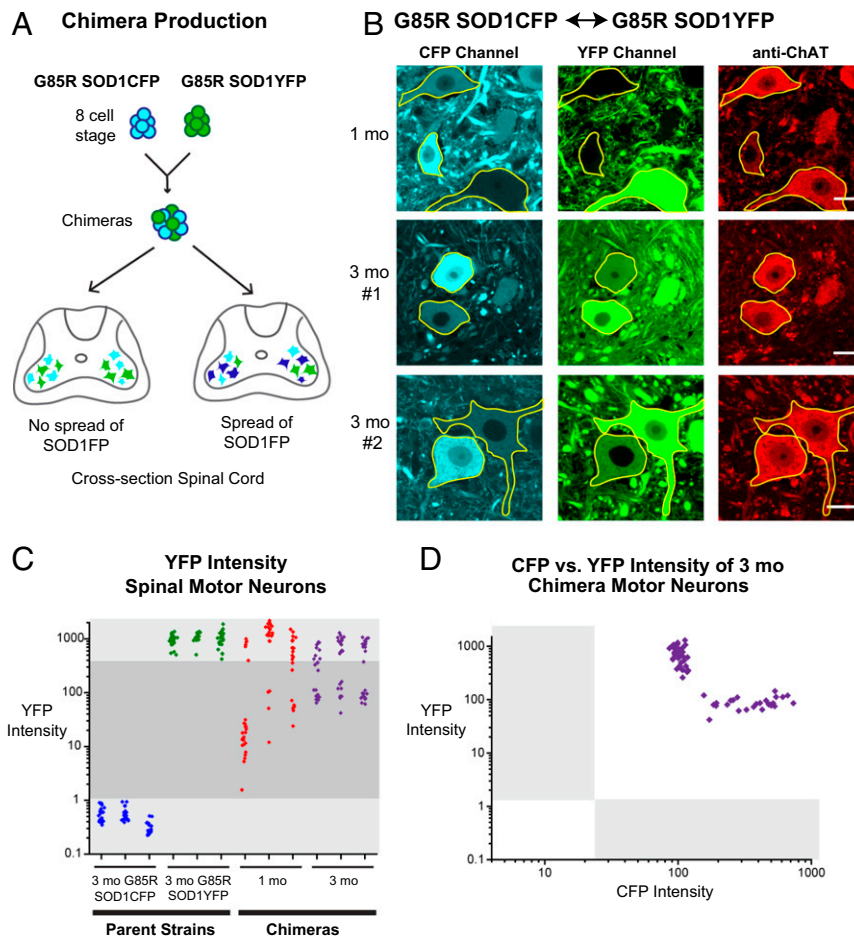
Fig. 1. Generation and analysis of G85R SOD1CFP↔G85R SOD1YFP chimeric mice. (*A*) Scheme for chimera production. Chimeras were produced from G85R SOD1CFP and G85R SOD1YFP "parental" transgenic ALS strains by aggregating eight-cell embryos from each strain. Motor neurons from spinal cord ventral horns of adult chimeras were analyzed to determine whether they exhibited only single fluorescence (no spread, cyan or green neurons, *Left*) or double fluorescence (spread, dark blue signifies double fluorescence, *Right*). (*B*) Representative confocal images from the lumbar spinal cord of three chimeric mice, one at 1 mo of age (*Top*) and two at 3 mo of age (*Middle* and *Bottom*). Motor neurons were identified with anti-ChAT antibody (red, *Right*; motor neurons outlined in yellow), and G85R SOD1CFP and G85R SOD1YFP are shown in the CFP (cyan) and YFP (green) channels, respectively. (Scale bars, 20 μm.) (*C*) Average YFP intensity per unit area (gray-scale values per square micrometer; 12-bit images) was measured for all motor neuron cell bodies (>20 μm diameter) detected in two sections of the lumbar spinal cord (20–25 cells) from each parental strain, G85R SOD1CFP ($n = 3$ mice, each mouse a vertical field of blue points, with each point representing one motor neuron) and G85R SOD1YFP ($n = 3$ mice; green points), and from chimeric mice aged 1 mo ($n = 3$ mice; red points) and 3 mo ($n = 3$ mice; purple points). The YFP intensity values of motor neurons in the G85R SOD1CFP parent strain (blue points), effectively a background measurement, are in the lower light-shaded region. The YFP intensity values of motor neurons in the G85R SOD1YFP parent strain (green points), a control for expressing motor neurons, are shown in the upper light-shaded region. Shaded in dark gray are the intensities of motor neurons lying between these reference values, which presumably comprise motor neurons that have received YFP fluorescence by transfer of G85R SOD1YFP from endogenously expressing cells. (*D*) CFP vs. YFP intensities are plotted for the same motor neurons of 3-mo-old chimeric mice as those shown in *C* (purple points), with each point representing an individual motor neuron. The light-gray shaded regions represent the background of YFP fluorescence in the G85R SOD1CFP transgenic parent (along the *x* axis) and the background of CFP fluorescence in the G85R SOD1YFP transgenic parent (along the *y* axis). Two groups of cells are apparent: high YFP, lower CFP and high CFP, lower YFP. Significantly, all motor neurons observed showed presence of the other fluorescent protein.

and contains a YFP coding sequence fused to the C-terminal SOD1 codon. This strain has high expression of the fusion protein in spinal cord motor neurons (producing strong cytosolic YFP fluorescence), develops large brightly fluorescent SOD1YFP aggregates in motor neurons as early as 1 mo of age, and paralyzes uniformly by 6 mo of age. G85R SOD1CFP transgenic mice were produced to serve as a chimera partner with a distinguishable fluorescence reporter and contain the same arrangement of the transgene, with CFP substituted for YFP. Similar to their partner, these mice exhibit bright cytosolic (CFP) fluorescence, develop SOD1CFP aggregates, and paralyze by 7–9 mo of age.

Transfer of G85R SOD1FPs Between Spinal Cord Motor Neurons. Spinal cord cross-sections from G85R SOD1YFP↔G85R SOD1CFP chimeras were analyzed by confocal microscopy at 1 and 3 mo of age.

Sections from the individual parental G85R SOD1FP strains were used to determine appropriate imaging settings, such that fluorescence in the YFP or CFP channel was independent of fluorescence in the other channel (Fig. S1*A*). At 1 mo of age, spinal motor neurons in chimeric mice, identified with anti-choline acetyltransferase (anti-ChAT) antibody, were observed to be brightly fluorescent for either CFP or YFP (Fig. 1*B*), with a much lower amount of fluorescence from the other protein, detectable only by intensity measurements (see below). By 3 mo of age, however, all spinal cord motor neurons in lumbar, thoracic, and cervical levels in chimeric animals were observed to contain both fluorescent proteins, one of considerable brightness (presumed to be the endogenously expressed protein) and the other of lesser intensity (presumed to comprise transferred protein) (Fig. 1*B*, *Middle* and *Bottom*). Notably, motor neuron processes also appeared to be doubly fluorescent.

Cytosolic fluorescent intensity measurements of motor neuron soma (here and subsequently) confirmed the observed relative intensities in the doubly fluorescent motor neurons in the 3-mo-old chimeric ventral horns (Fig. 1C, purple points). One group of motor neurons (above the dark-gray box in Fig. 1C) had intensity values comparable to those observed in motor neurons from the parental G85R SOD1YFP strain (Fig. 1C, green points). These are apparently motor neurons endogenously expressing G85R SOD1YFP. A second group of motor neurons (within the gray box in Fig. 1C) had lesser YFP intensity values, but these values were 40- to 100-fold greater than background YFP intensity in motor neurons of the parental G85R SOD1CFP strain (Fig. 1C, blue points). This second group of motor neurons, all themselves exhibiting strong CFP intensity, apparently corresponded to a population that received G85R SOD1YFP by transfer from motor neurons endogenously expressing this protein. Intensity measurements in motor neurons at one month of age (Fig. 1C, red points) showed a similar distribution into two groups, although the fluorescence intensity of the transferred G85R SOD1YFP (dark-gray box in Fig. 1C) was generally lower than at 3 mo, but still well above the background.

The foregoing interpretation of the relative intensities in the doubly fluorescent motor neurons was supported by plotting YFP intensity vs. CFP intensity for the motor neurons from the 3-mo-old chimeras shown in Fig. 1C (Fig. 1D). Only two populations were observed: cells with a high intensity of YFP and a relatively low intensity of CFP, and cells with a high intensity of CFP and relatively low intensity of YFP. Notably, motor neurons with high (i.e., parental) intensity of both G85R SOD1YFP and G85R SOD1CFP were not observed. The intensity data thus support that doubly fluorescent neurons have high fluorescence intensity produced from the endogenously expressed protein and lower fluorescence from the other fluorescent protein as a result of transfer from neurons expressing it.

Does the apparent transfer of mutant SOD1 fluorescent protein between spinal cord motor neurons reflect a more general behavior of neurons that can be observed elsewhere in the CNS? To assess this, three different regions of the CNS were examined in detail in 3-mo-old chimeric mice: layer V of the motor cortex (Fig. S1B), the CA1 region of the hippocampus (Fig. S1B), and the dorsal horn of the spinal cord. In all three locations, only YFP or CFP fluorescence was observed in these neurons, with a complete absence of fluorescence ("black hole" in images) at the position of the neuron somata expressing the other fluorescent protein.

Aggregates of G85R SOD1FP Do Not Transfer Between Motor Neurons. Transfer of aggregated mutant SOD1 between motor neurons has been hypothesized to contribute to spread of SOD1 motor neuron pathology within the spinal cord (e.g., refs. 15 and 17). The chimeric mice offered an opportunity to inspect for transfer of aggregates generated endogenously within mutant SOD1 motor neurons, avoiding exogenous addition or injection of aggregated material. Notably, aggregate formation in the G85R SOD1FP transgenic strains is confined to cell bodies, with EM evidence suggesting that small cytosolic aggregates grow and coalesce into the observed large fluorescent structures that are up to 20–30 μm in diameter. Approximately 300 aggregates in motor neuron cell bodies of 3-mo-old chimeric mice were scored in both the YFP and CFP channels (Fig. S2A), including z-stack analysis of ~50 such aggregates. In all cases, this revealed single fluorescent signals in the aggregate that corresponded exactly to the endogenously expressed fluorescent protein (Fig. S2A and sample images in Fig. S2 B and C). Although we uniformly observed fluorescence from the transferred protein in the cytosol of these cell bodies, the transferred protein was not detected in the aggregate. As evidence that coaggregation of the two fluorescent G85R SOD1's can occur, a retrograde transduction experiment was carried out, injecting recombinant AAV6 expressing CMV-driven G85R SOD1CFP into the tibialis anterior (TA) muscle of

4-d-old G85R SOD1YFP mouse pups. Here, retrograde transport of the virus to the innervating TA motor neuron pool in the lumbar spinal cord led to strong expression of G85R SOD1CFP in these neurons at 3 mo of age and, in this context, we observed doubly fluorescent coaggregates (Fig. S2D). Thus, transfer between motor neurons appears to involve soluble G85R SOD1 species, and insoluble aggregate material does not transfer. Moreover, it also seems that transferred protein does not detectably accrete in the aggregates.

A Wild-Type SOD1YFP Fusion Protein Transfers. Was transfer in the G85R SOD1YFP↔G85R SOD1CFP chimeric mice dependent on misfolding of the mutant SOD1 moiety of the fusion protein, or could folded, dimeric, wild-type SOD1YFP (87 kDa) (described in ref. 20) also be transferred? To address this question, we produced wtSOD1YFP↔G85R SOD1CFP chimeras. In 3-mo-old mice, we observed transfer of both fluorescent species (Fig. 2A). Most importantly, G85R SOD1CFP-expressing cells displayed YFP fluorescence from transferred wtSOD1YFP. The level of cytosolic fluorescence in the setting of transfer relative to that of endogenously expressing wtSOD1YFP neurons was determined by measuring cytosolic fluorescence intensity per square micrometer. The intensity of fluorescence from the transferred wtSOD1YFP reached a level ~50% that of endogenously expressing cells. The relatively strong accumulation of transferred wtSOD1YFP may reflect the stability of wtSOD1YFP, which has been observed in vivo in spinal cord to turn over at a rate approximately one-tenth that of G85R SOD1YFP (half-life of ~20 d vs. ~2 d) (21). The transfer of wtSOD1YFP indicates that the mechanism of transfer does not depend on cell toxicity and death, as produced by G85R SOD1YFP, because wtSOD1YFP produces no symptoms or detectable cell loss in the parent strain.

An mCherry Protein Targeted to Mitochondria Does Not Transfer. Because an ~87-kDa wtSOD1YFP dimer could transfer between motor neurons, we asked whether an entire organelle, such as a mitochondrion, can be transferred. There is precedent from oogenesis in *Drosophila* for such transfer between cells via so-called ring canals (22). To test for such transfer, a chimera was formed between a strain transgenic for Thy1.2 promoter-driven mitochondrial-targeted mCherry (Thy1.2P-mito-mCherry) and the G85R SOD1YFP strain. When spinal cord motor neuron cell bodies of G85R SOD1YFP-expressing cells were examined for mito-mCherry, none were observed (Fig. 2B). These data indicate that mitochondria are not transferred between motor neurons. The findings also indicate that transfer does not occur at the mRNA level because, if it did, the transferred mRNA would be expected to direct translation of mito-mCherry in recipient cells. In contrast to the lack of transfer of mito-mCherry to G85R SOD1YFP-expressing cells, G85R SOD1YFP was transferred to the mito-mCherry–expressing cells, observed by microscopy (Fig. 2B) and by YFP intensity measurements (Fig. 2C). Transfer in this context indicates that there is no requirement for a motor neuron receiving G85R SOD1YFP to itself express such a fusion protein. This chimera also afforded an opportunity to assure that the misfolded human G85R SOD1 moiety of the G85R SOD1YFP fusion protein is transferring: that is, that the intact fusion protein is transferring, as opposed to simply the YFP moiety, because there is no endogenous misfolded human SOD1 expressed in the mCherry^{+} cells. An antibody that specifically recognizes misfolded human SOD1 and not mouse SOD1 (23) showed positive cytosolic signals in the mCherry^{+} motor neurons, confirming the presence of the human SOD1 moiety in the transferred protein.

EGFP Alone Transfers Between Motor Neurons. The observation that wtSOD1YFP, a native, nonpathogenic protein, could transfer between motor neurons raised the question as to whether cytosolic proteins, more generally, could transfer between motor neurons.
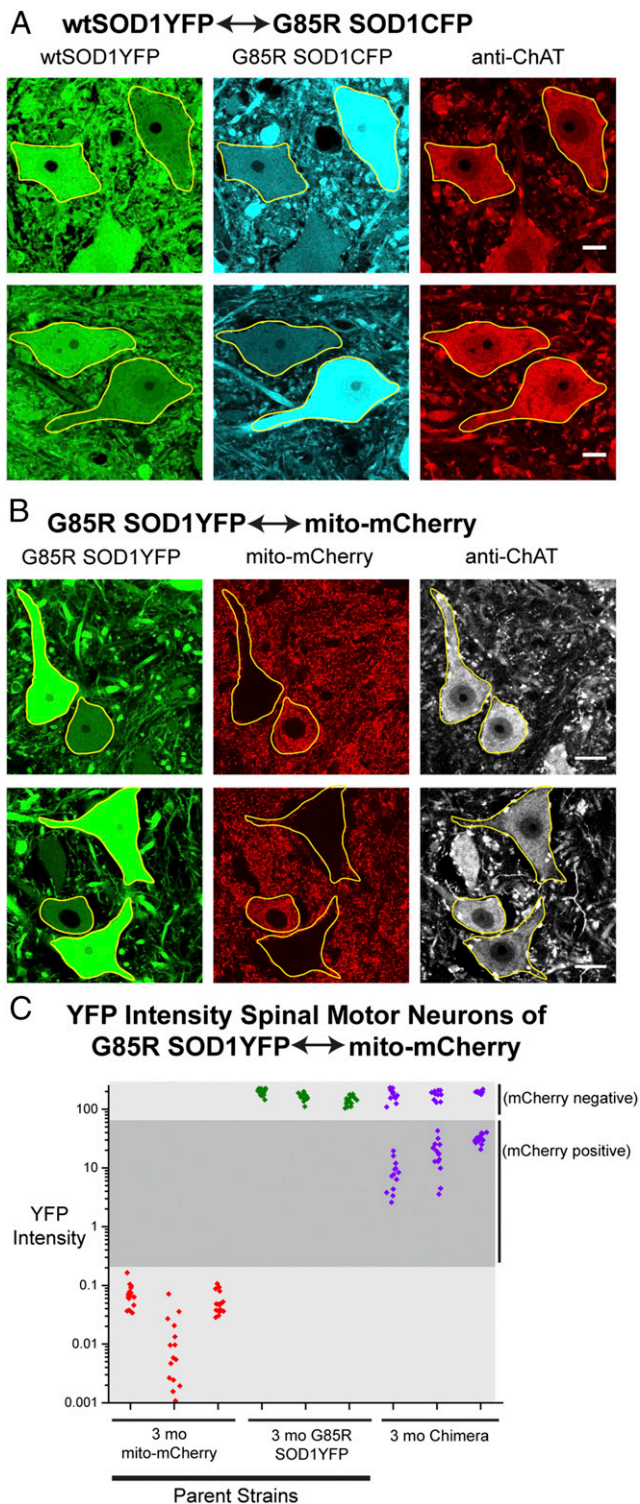
Fig. 2. Transfer of a nonpathogenic wild-type SOD1YFP protein, but not organelles. (*A*) Representative lumbar spinal cord sections from two wtSOD1YFP↔G85R SOD1CFP chimeras. Motor neurons in lumbar spinal cord sections were labeled with anti-ChAT antibody and imaged by confocal microscopy; neurons are outlined in yellow. (Scale bars, 20 μm.) Transfer of wtSOD1YFP (nonpathogenic) is apparent. (*B*) Lumbar spinal cord sections of two G85R SOD1YFP↔Thy1.2P-mito-mCherry chimeras. Motor neurons are identified by staining with anti-ChAT antibody (outlined in yellow, *Right*). (Scale bars, 20 μm.) Transfer of cytosolic G85R SOD1YFP into mito-mCherry⁺ cells occurs, but transfer of mitochondrially targeted mCherry into G85R SOD1YFP-expressing cells does not occur. (*C*) YFP fluorescence intensities (gray-scale values per square micrometer; 8 bit) in

To answer this question, a chimera was formed between strains transgenic for ChAT promoter-driven EGFP (ChAT[P]-EGFP) and Thy1.2[P]-mito-mCherry. When spinal cords of 3-mo-old chimeras were examined, robust transfer of EGFP was observed into mito-mCherry–expressing motor neurons (Fig. 3*A*). The intensity of the transferred protein was ~50% that in the endogenously EGFP-expressing cells, perhaps reflecting the efficiency of transfer of EGFP. By measuring the intensity of the transferred EGFP fluorescence in six chimeric mice with different percentages of EGFP⁺ donor motor neurons, we observed that, in general, the greater the percentage of EGFP-donor neurons, the greater the intensity of EGFP in the mito-mCherry⁺ recipient neurons (Fig. 3*B*). This finding could be consistent with local transfer simultaneously occurring from multiple surrounding motor neurons, such that the greater the number of surrounding EGFP-expressing (donor) motor neurons, the more EGFP that could be transferred into any given (recipient) mito-mCherry⁺ motor neuron.

Absence of Transfer Between Motor Neurons in Extraocular Cranial Nerve Motor Nuclei. In cases of human ALS, there is relative sparing of extraocular muscles, innervated by cranial motor nuclei 3N (oculomotor), 4N (trochlear), and 6N (abducens). This finding contrasts with pathologic effects on other cranial motor nuclei, 5N (motor nucleus of trigeminal), 7N (facial), and 12N (hypoglossal). Was there any correlation of these findings with the ability of EGFP to transfer between motor neurons within the cranial nerve motor nuclei? To assess this question, we examined the brainstem cranial nerve motor nuclei in the ChAT[P]-EGFP↔Thy1.2[P]-mito-mCherry chimera just described (Fig. 4). Representative images show detection of GFP fluorescence in mito-mCherry⁺ recipient cells in 5N and 7N, but no GFP fluorescence in mito-mCherry⁺ cells in 3N or 4N (Fig. 4*A*). GFP intensity measurements were carried out in mCherry⁺ motor neurons from three different chimeric mice and compared with the background intensity in the GFP channel in 7N of the mito-mCherry⁺ parent strain (Fig. 4*B*). Whereas robust intensity is observed in mito-mCherry⁺ (recipient) cells in the 5N, 7N, and 12N motor neurons, no intensity above background was observed in 3N, 4N, or 6N. Thus, in the clinically spared extraocular motor nuclei, we observed no transfer of cytosolic EGFP between motor neurons. This finding suggests that whatever mechanism or structure might be involved in transfer of a cytosolic protein between motor neurons, it is absent in the extraocular cranial nerve motor nuclei and might contribute to clinical sparing.

Apparent Transfer of EGFP from Motor Neurons to Nearby Oligodendrocytes. During analysis of the ChAT[P]-EGFP transgenic strain and its chimera, we noticed small, strongly GFP-fluorescent cell bodies, less than 10-μm diameter, in close proximity to motor neurons in the gray matter of the ventral spinal cord (Fig. 5*A*). To identify these EGFP-containing cells, tissue sections were immunostained for markers of glial cells, including Olig2, Sox10, GFAP, and Iba1. Neither astrocytes (GFAP⁺) nor microglia (Iba1⁺) showed GFP fluorescence.

lumbar motor neurons of G85R SOD1YFP↔Thy1.2[P]-mito-mCherry chimeras (*n* = 3 mice; purple points) at 3 mo of age and parental donor strains, Thy1.2[P]-mito-mCherry mice (*n* = 3 mice; red points) and G85R SOD1YFP mice (*n* = 3 mice; green points). Shaded in light gray, lower, are YFP intensity values of the Thy1.2[P]-mito-mCherry parental strain (red points; background level) and of G85R SOD1YFP endogenously expressing cells in the parental G85R SOD1YFP strain (green points, upper light-gray region), as well as mCherry⁻ G85R SOD1YFP expressing motor neurons of the chimeras (purple points). Shaded in dark gray are those values determined for mito-mCherry–expressing motor neurons in the chimeras that have received G85R SOD1YFP, with intensity values intermediate to the parental strains. These motor neurons had intensities 10–100× greater than background, but were ~10% the value of the parental G85R SOD1YFP motor neurons.

Only oligodendrocyte-lineage cells, marked with Olig2 and Sox10 antibodies, were EGFP fluorescent (Fig. 5 *A* and *B*). To further distinguish these cells along the oligodendrocyte lineage, sections were stained with antibodies recognizing mature oligodendrocytes (CNPase, CC1), immature oligodendrocytes (O4), or progenitor cells (NG2, PDGFRα). Antibodies recognizing mature oligodendrocytes colocalized with EGFP (see, for example, Fig. 5*C*),
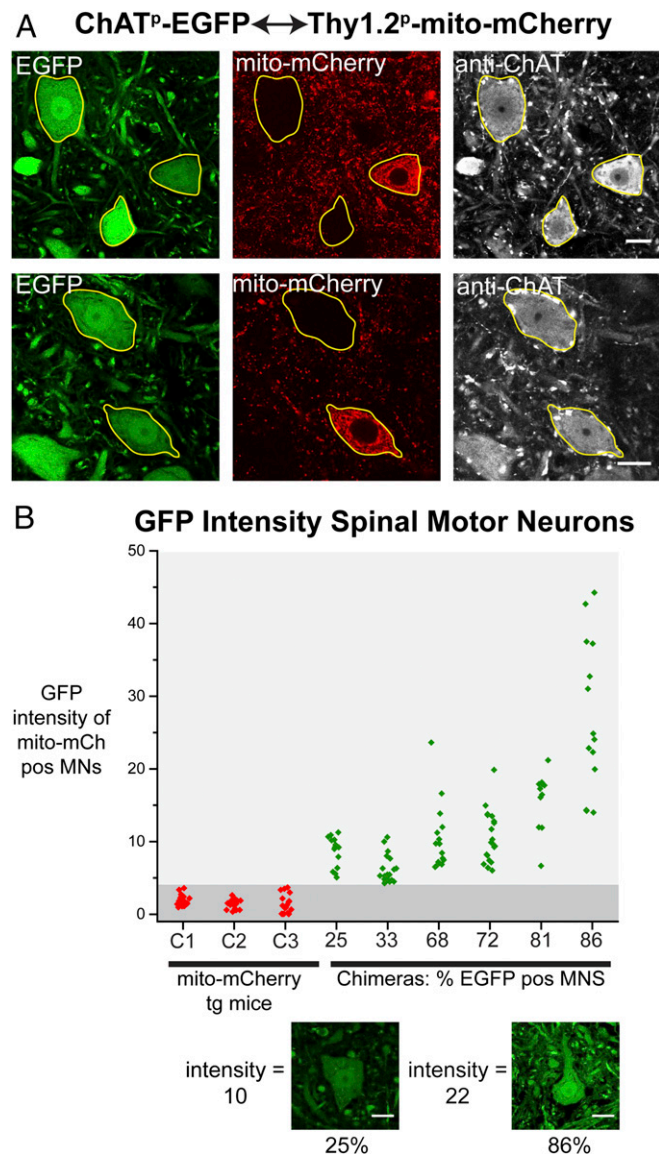
whereas antibodies to progenitor cells and immature oligodendrocytes did not identify cells that contained EGFP (see, for example, Fig. 5*D*). These results suggest that EGFP expressed in motor neurons can be transferred to neighboring mature oligodendrocytes. A time-course analysis supported a temporal progression of transfer, with staining with anti-CC1, Olig2, and Sox10 each indicating increasing numbers of GFP-costaining cells (see Fig. S3*A* for plots and Fig. S3*B* for anti-CC1 images), with 40–80% of gray matter oligodendrocytes exhibiting GFP fluorescence by 84 d. Because it is possible that low-level expression from the ChAT promoter could produce EGFP in mature oligodendrocytes, we used a construct with a second promoter to further assess whether transfer was occurring.

The Thy1.2 promoter serves as a general neuronal promoter (24). Notably, in both the parental Thy1.2^P-mito-mCherry mice and the Thy1.2^P-mito-mCherry↔ChAT^P-EGFP chimeras, we did not observe any mCherry fluorescence in the oligodendrocytes that had been identified with anti-Olig2 or anti-Sox10 (Fig. S4*A*). This finding indicates that the Thy1.2 promoter does not drive expression to a detectable extent in oligodendrocytes. It also reflects that the fluorescent mitochondria in mito-mCherry–expressing motor neurons do not transfer to oligodendrocytes, analogous to the result that they do not transfer between motor neurons (Figs. 2 and 3). In contrast, YFP expressed in the cytosol of motor neurons from the Thy1.2 promoter appears to transfer over time to nearby oligodendrocytes (Fig. S4 *B* and *C*). In particular, at 14 d the YFP-fluorescent neurons and CC1$^+$ oligodendrocytes (the latter in red in Fig. S4*C*) are distinct from each other; at 28 d, some oligodendrocytes show colocalization (yellow in the merged image), and by 84 d they are nearly all yellow. This result appears to reflect a temporal trajectory of transfer from motor neurons to oligodendrocytes.

Transfer of SOD1FP Fusion Proteins from Motor Neurons to Nearby Oligodendrocytes. We examined the SOD1FP chimeras, G85R SOD1YFP↔G85R SOD1CFP and wtSOD1YFP↔G85R SOD1CFP, to determine whether these fusion proteins could also transfer to oligodendrocytes. In particular, the presence of both fluorescent proteins in oligodendrocytes of chimeric mice would support the conclusion that, at a minimum, one fluorescent protein had been acquired exogenously. Both fluorescent proteins were indeed visually observed in many Olig2$^+$ cells in the ventral horns of the 3-mo-old chimeras. With intensity measurements, >90% of oligodendrocytes in the ventral horn of lumbar spinal cord sections of both chimeras contained detectable amounts of both fluorescent proteins. Plotting cytosolic CFP intensity vs. YFP intensity on an individual cell basis revealed that oligodendrocytes contained a widely variable amount of the two fluorescent proteins, including oligodendrocytes with high intensity of both proteins, low intensity of both proteins, and with high intensity of one and low of the other (Fig. S5*A*). Within any given small region of the ventral horn, all of these possibilities were evident. The varying amounts of fluorescent protein may reflect oligodendrocytes at different temporal stages of acquiring SOD1FP. Unlike oligodendrocytes in the gray matter of the spinal cord, oligodendrocytes in the cortex (layer V) and in the corpus callosum apparently do not receive SOD1FP; they exhibited only single fluorescence, presumably expressed endogenously from the SOD1 promoter (Fig. S5 *B* and *C*).

Temporally Observed Transfer from Motor Neurons to Oligodendrocytes in a Retrograde Labeling Experiment. Is there a time-dependence to the transfer of proteins from neurons to oligodendrocytes? To address this question, a retrograde transduction experiment was carried out, injecting a recombinant AAV6 expressing wtSOD1CFP into the TA muscle in the hindlimb of a B6/SJL mouse at postnatal day 4 (P4). The virus is transported retrogradely up axons to the lumbar TA motor neuron pool, where episomal viral genomes drive stable wtSOD1CFP expression (25) (Fig. 6*A*). By 11 d

Fig. 3. Transfer of EGFP to motor neurons in ChAT^P-EGFP↔Thy1.2^P-mito-mCherry chimeric mice. (*A*) Representative sections of lumbar spinal cord from two different ChAT^P-EGFP↔Thy1.2^P-mito-mCherry chimeric mice stained with anti-ChAT antibody and analyzed by confocal microscopy. (Scale bars, 20 μm.) Transfer of EGFP to mito-mCherry–expressing motor neurons is apparent. (*B*) Intensities (gray-scale values per square micrometer; 8 bit) in the GFP channel of all motor neurons from two cross-sections of lumbar spinal cord of six ~3-mo-old chimeric mice (green points) with varying percentage of EGFP$^+$ (mito-mCherry$^-$) motor neurons (indicated on the x axis) and three mice of the parental Thy1.2^P-mito-mCherry transgenic strain (C1, C2, C3, red points). Below are representative images from two different chimeric mice of mito-mCherry$^+$ motor neurons receiving EGFP, one from a mouse with 25% EGFP-expressing/75% mito-mCherry–expressing cells, with a GFP intensity of 10 (*Left*), and one from a mouse with 86% EGFP-expressing/14% mito-mCherry–expressing cells and a higher GFP intensity value of 22 (*Right*). (Scale bars, 20 μm). This could suggest that motor neurons can receive cytosolic protein from more than one other motor neuron.

postinjection (P15), motor neurons in the L4/5 TA motor pool region of the spinal cord were CFP-fluorescent (Fig. 6 *B* and *D*). At 11 and 14 d postinjection, whereas 32–83% of motor neurons were CFP-fluorescent, essentially no CFP-fluorescent Olig2$^+$ oligodendrocytes were observed in their neighborhood (Fig. 6*D*). By 21 d, occasional Olig2$^+$ oligodendrocytes displayed

Absence of transfer in extraocular cranial motor nuclei

A   ChAT^P-EGFP⟷Thy1.2^P-mito-mCherry
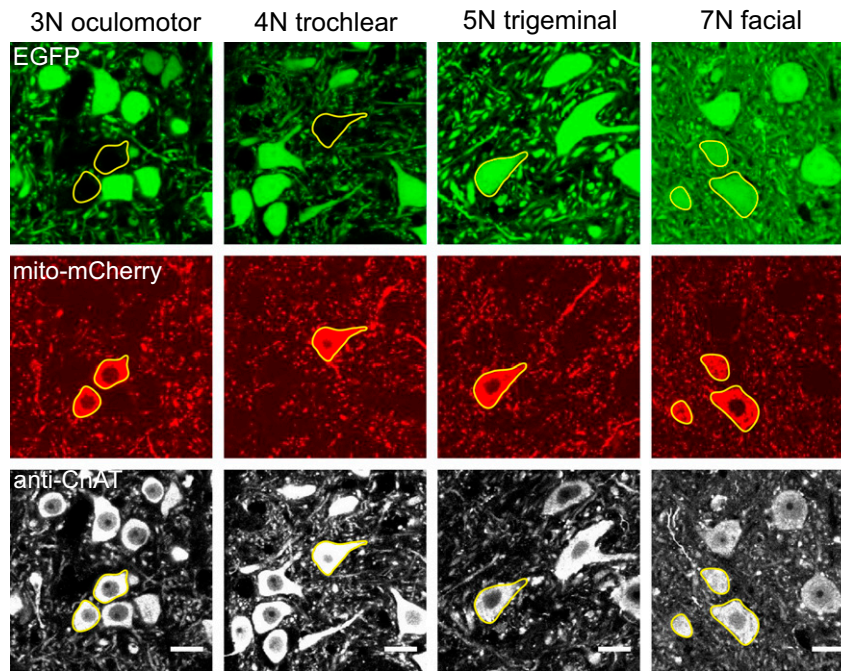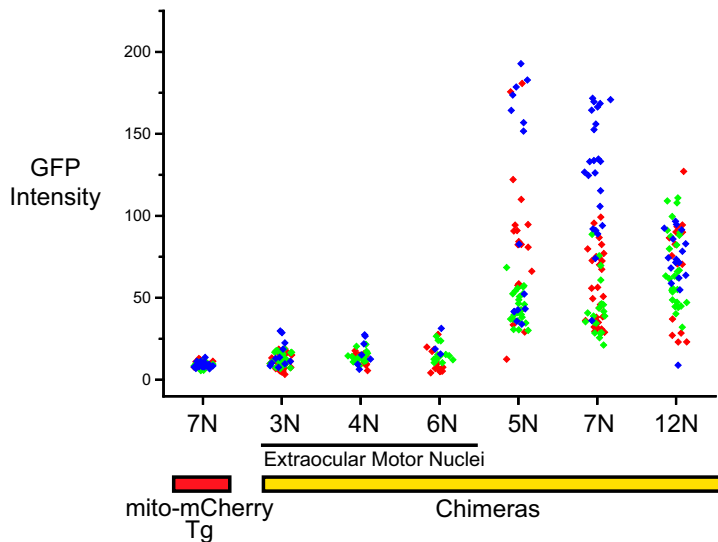
Fig. 4. Absence of transfer in extraocular cranial motor nuclei, spared in ALS. (*A*) Representative confocal images from the brainstem of a ChAT^P-EGFP↔Thy1.2^P-mito-mCherry chimeric mouse. Sections containing cranial motor nuclei—3N (oculomotor), 4N (trochlear), 5N (trigeminal), and 7N (facial)—were stained with anti-ChAT antibody to label motor neurons in each nucleus (*Bottom*). All mito-mCherry$^+$ motor neurons (*Middle*) are outlined in yellow. (Scale bars, 20 μm.) Note the absence of EGFP in mito-mCherry–expressing neurons in 3N and 4N, but its presence in 5N and 7N (*Top*). This difference in transfer correlates with sparing vs. susceptibility of the respective cranial nerve nuclei in ALS patients. (*B*) Intensities (gray-scale values per square micrometer; 8 bit) calculated from 3N, 4N, 6N (extraocular nuclei), and 5N, 7N, and 12N from chimeric mice (*n* = 3 mice) and from 7N of Thy1.2^P-mito-mCherry parent mice as a control (*n* = 3 mice). Each point represents a single motor neuron, and the values for motor neurons from individual mice are colored red, green, or blue. Intensity values from nuclei involved in extraocular eye movements (spared in ALS patients) are similar in value to the background cell intensity measurements in 7N of Thy1.2^P-mito-mCherry control mice, indicating no transfer, whereas many motor neurons in 5N, 7N, and 12N, affected in ALS, have higher intensity values consistent with transfer. Note that there was variation in the level of transfer in cranial nerve nuclei 5N, 7N, and 12N within a given mouse and from mouse to mouse.

CFP fluorescence; by 28 d, 1–6% of oligodendrocytes were CFP$^+$, and by 42 d, 4–16% were positive (Fig. 6 C and D). At 140 d, an even greater percentage of CFP$^+$ oligodendrocytes (up to 33%) was observed. The ratio of CFP-fluorescent oligodendrocytes to CFP$^+$ motor neurons in the TA motor pool also steadily increased (Fig. 6D, right-hand column). Thus, this kinetic analysis reveals
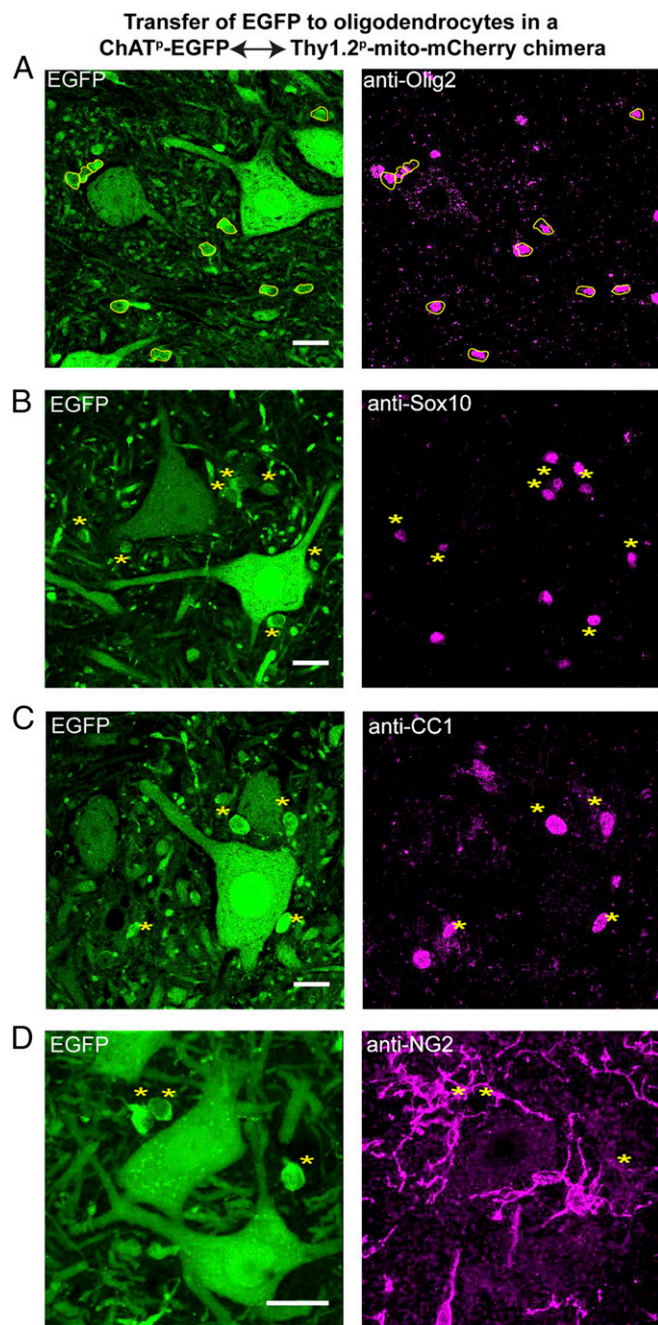

Fig. 5. EGFP observed in oligodendrocytes in ChAT^p-EGFP→Thy1.2^p-mito-mCherry chimeric mice. Spinal cord cross-sections from 3-mo-old ChAT^p-EGFP↔Thy1.2^p-mito-mCherry chimeric mice stained with antibodies against Olig2 (A), Sox10 (B), CC1 (C), and NG2 (D). Single optical slices are shown for A–C; a projection image of a z-stack is shown for D. (Scale bars, 20 μm.) Small cells that are EGFP$^+$ are circled in yellow in A and indicated by asterisks in B–D. Coincidence of EGFP fluorescence with anti-Olig2 and anti-Sox10 staining indicates that these are oligodendrocyte lineage cells, and anti-CC1 staining (C) further identifies the cells as mature oligodendrocytes. (D) There is no staining of the cells with anti-NG2, a marker for oligodendrocyte precursors. See also Figs. S3–S5.

the appearance of CFP fluorescence first in motor neurons, by as early as 11 d postinjection, followed 17–31 d later by substantial acquisition of CFP fluorescence in oligodendrocytes, consistent with time-dependent transfer from motor neurons to oligodendrocytes. Notably, this resembles the temporal development of fluorescence in the oligodendrocytes of the transgenic ChAT^p-EGFP and Thy1.2^p-YFP mice (Figs. S3 and S4), but the percentage of receiving oligodendrocytes was substantially greater in the transgenic mice, reaching 38–66% of Olig2-labeled cells, likely the result of the greater density of fluorescent donor motor neurons in the transgenic mice.

Discussion

Spread of Cytosolic Proteins Between Motor Neurons. Producing chimeric mice by mixing eight-cell early mouse embryos from two donor mouse strains expressing two distinct fluorescent proteins has allowed observation, here in vivo in the derived adult mice, of the temporal spread of several cytosolic proteins, both pathogenic and nonpathogenic, between spinal cord motor neurons through detection of doubly fluorescent neurons. Such transfer seems to be confined to spinal cord motor neurons and to the motor neurons in cranial nerve nuclei affected in ALS. Significantly, spread was not observed in the extraocular cranial nerve nuclei, which are relatively spared in ALS, nor in other CNS regions, such as the hippocampus or motor cortex, where only singly fluorescent neurons were observed. This specificity may be a function of the motor neuron populations themselves or may depend on the nature of a physically neighboring mature oligodendrocyte population that also received these cytosolic proteins, which could serve as an intermediary in the transfer.

Transferred proteins included G85R mutant human SOD1 fused to YFP or CFP, but also wild-type SOD1 fused to YFP, and EGFP alone. Although the SOD1 proteins were overexpressed from high-copy transgenes, EGFP was expressed from a ChAT promoter, a moderately active promoter, at four copies per haploid genome. Concerning the protein products, wild-type SOD1YFP is a stable 87-kDa homodimeric protein, suggesting that average-sized proteins can be subject to transfer. Additional chimeras are being produced to test for transfer of other, including larger, protein species. For all of the proteins examined, transferred protein was detectable in recipient cells at a low level at 1 mo of age but increased by approximately an order-of-magnitude by 3 mo of age. Interestingly, the increase of transferred fluorescent proteins in recipient motor neurons parallels the development of fluorescence in neighboring mature (CC1$^+$, CNPase$^+$) oligodendrocytes (Fig. 5 and Figs. S3–S5) and parallels morphologic changes occurring in these oligodendrocytes across this time period (discussed below; see also Figs. S3 and S4).

Transfer appears to occur locally, as suggested by the increased receipt of transferred fluorescence with increased percentage of donor cells within the chimera (Fig. 3B), potentially reflecting that simultaneous transfer from multiple surrounding motor neurons can occur. In addition, one chimeric mouse exhibited a fluorescent "patch" of G85R SOD1CFP expression in an otherwise G85R SOD1YFP-expressing spinal cord. The distance of transfer from endogenously expressing motor neurons at the edges of the patch to neighboring recipient neurons was several hundred micrometers, with CFP fluorescence intensity decreasing with distance (Fig. S6). Notably, as many as 100 motor neurons could lie within such a radius. Whether longer distances could be traversed with greater time—for example, in the context of a human life span—and whether local "conversion" by transferred pathogenic species could be a means of propagating stable pathogenic species between distant motor neurons, remains to be determined. Notably, in contrast with the transfer of soluble cytosolic species, neither aggregated mutant SOD1FPs nor mitochondria were transferred.

Interestingly, cytosolic transfer of nonpathogenic proteins that seems to resemble the transfer observed here has recently

Fig. 6. Expression of wtSOD1CFP first in motor neurons after TA injection of AAV6 SOD1CFP, followed by transfer to oligodendrocytes. (*A*) Scheme of the kinetic experiment. P4 wild-type mice were injected in the TA muscle with AAV6 wtSOD1CFP. Lumbar spinal cord cross-sections were inspected for presence of CFP in motor neurons of the TA pool and neighboring oligodendrocytes at various times postinjection. Transduced motor neurons with CFP fluorescence were first visible in the spinal cord TA motor pool at 11 d. L5 spinal cord cross-section of an 11-d-old (*B*) and a 42-d-old (*C*) mouse that had been injected with AAV6 wtSOD1CFP, both stained with anti-Olig2 antibody (magenta). No CFP fluorescence is visible in oligodendrocytes at 11 d, but many show cytoplasmic CFP fluorescence at 42 d. Note that Olig2 is localized to the nucleus. (Scale bars, 20 μm.) (*D*) Table summarizing transfer of wtSOD1CFP to oligodendrocytes in 19 mice injected in TA muscle with AAV6 wtSOD1CFP. The number of CFP+ motor neurons (ChAT stained) and oligodendrocytes (Olig2 stained) in the nidus of viral transduction in L5 were counted, along with the total numbers of both motor neurons and oligodendrocytes. The ratio of CFP-containing oligodendrocytes to CFP-expressing motor neurons (last column) increases with time after injection, reflecting time dependent transfer of wtSOD1CFP from neurons to oligodendrocytes.

been reported to occur between retinal photoreceptor cells in the context of transplantation experiments injecting fluorescently labeled donor photoreceptor cells into the subretinal space of adult wild-type mice (26–28). Transfer of cytosolic proteins—GFP, cre recombinase, and α-transducin—was observed between donor photoreceptor cells and the neighboring host photoreceptors, and transfer appeared to occur bidirectionally, taking place in the absence of nuclear transfer/fusion.

As concerns the motor system, why would motor neurons "talk" with each other at the cytosolic level, exchanging at least some fraction of protein species? Perhaps this is a means of setting a shared local physiology within a motor neuron pool that would support commonality of metabolic, electrical, or other signaling

systems. It could allow as well for dissipation of toxic protein species formed in one or more neurons by transfer to the neighbors. Alternatively, transfer between motor neurons may be a consequence of back-and-forth cytosolic transfer between motor neurons and neighboring mature oligodendrocytes, as discussed below, the latter of which may provide not only myelination function but additional supportive roles to motor neurons. There is a precedent for beneficial cross-talk between oligodendrocytes and motor axons, with the oligodendrocyte monocarboxylate transporter MCT1 enabling export of lactate from oligodendrocytes as a local energy source (29). Clearly, experiments blocking the protein transfer process will be informative concerning its normal and pathogenic roles.

Mature Oligodendrocytes as a Potential Mediator of Protein Transfer. The observation of transfer of fluorescent proteins into mature oligodendrocytes neighboring motor neurons in the spinal cord gray matter, with a temporal increase that parallels that of protein transfer between motor neurons, makes it inescapable to consider that oligodendrocytes serve as a vehicle for transfer between motor neurons. Although transfer in a direction from motor neurons to oligodendrocytes seems supported, particularly from a kinetic experiment (Fig. 6), transfer in turn from oligodendrocytes to motor neurons is less clear. We have preliminarily observed, however, that in transgenic Olig2P-GFP mice, there is progressive transfer of GFP from spinal cord oligodendrocytes to motor neurons and also, selectively, from oligodendrocytes in ALS-affected cranial nerve motor nuclei to neighboring motor neurons, supporting that such transfer can occur and follows the same selectivity observed for transfer between motor neurons (Fig. S7). However, definitive support for oligodendrocyte involvement in sequential transfer from and to motor neurons will require further kinetic observations or an oligodendrocyte ablation experiment.

The question remains as to the precise mechanism of cell–cell transfer, but we speculate that oligodendrocyte processes might be involved. These fine processes appear to contact motor neuron cell bodies and appear to expand their interaction across the 4- to 8-wk period during which transfer increases to a very noticeable level (we note also that oligodendrocyte cell bodies appear to become reduced in volume during this same time). How such processes could transfer protein from/to motor neuron processes or somata remains unclear, but involvement of extrasynaptic junctions/pores or exovesicles are considerations.

Whatever the mechanism, we note that oligodendrocytes elsewhere in the nervous system do not seem to participate in transfer, as they fail to exhibit the double fluorescence observed in spinal cord gray matter oligodendrocytes (Fig. S5). This different behavior correlates with the different origins of oligodendrocytes of the spinal cord and brain, in the former case from floorplate (30) and in the latter from multiple locations in waves (31). In contrast, motor neurons and oligodendrocytes in the spinal cord share a common embryonic source (32, 33). Perhaps this developmental connection determines the physical connection that becomes apparent in adult life.

Finally, an involvement of ventral gray matter oligodendrocytes in pathogenesis of SOD1-linked ALS is supported by several recent studies (34–36). Both early-onset turnover of mature oligodendrocytes themselves, with activated precursor proliferation/differentiation, and toxicity conferred by dysfunctional oligodendrocytes upon motor neurons were reported. Reduction of SOD1 in oligodendrocytes was able to delay onset of SOD1-linked ALS in a transgenic mouse strain (34). The finding here of transfer of mutant SOD1 and putatively other cytosolic proteins to oligodendrocytes, and the potential of oligodendrocytes to transfer cytosolic proteins to motor neurons could add a further level of understanding to these observations.

Further studies of the population of mature gray matter oligodendrocytes should better define their role in motor neuron maintenance in health and disease. Whether these cells are migratory and capable of serving as a delivery vehicle to distant motor neurons is of interest. Also of interest is the mechanism of protein transfer and whether it involves particular structures that, for example, would be specifically present in ALS-affected cranial nerve motor nuclei and absent from the relatively spared extraocular nuclei.

Materials and Methods

Animals. All animal experiments were carried out under protocols approved by the Yale University Institutional Animal Care and Use Committee in accordance with National Institutes of Health guidelines for the ethical treatment of animals.

Methods. Other methods are detailed in SI Materials and Methods, and antibodies used and conditions for immunostaining are listed in Table S1.

1. Jucker M, Walker LC (2013) Self-propagation of pathogenic protein aggregates in neurodegenerative diseases. *Nature* 501:45–51.
2. Collinge J (2016) Mammalian prions and their wider relevance in neurodegenerative diseases. *Nature* 539:217–226.
3. Braak H, Braak E (1991) Neuropathological stageing of Alzheimer-related changes. *Acta Neuropathol* 82:239–259.
4. Brandner S, et al. (1996) Normal host prion protein (PrP^C) is required for scrapie spread within the central nervous system. *Proc Natl Acad Sci USA* 93:13148–13151.
5. Braak H, et al. (2003) Staging of brain pathology related to sporadic Parkinson's disease. *Neurobiol Aging* 24:197–211.
6. Kordower JH, Chu Y, Hauser RA, Freeman TB, Olanow CW (2008) Lewy body-like pathology in long-term embryonic nigral transplants in Parkinson's disease. *Nat Med* 14:504–506.
7. de Calignon A, et al. (2012) Propagation of tau pathology in a model of early Alzheimer's disease. *Neuron* 73:685–697.
8. Ravits JM, La Spada AR (2009) ALS motor phenotype heterogeneity, focality, and spread: Deconstructing motor neuron degeneration. *Neurology* 73:805–811.
9. Rosen DR, et al. (1993) Mutations in Cu/Zn superoxide dismutase gene are associated with familial amyotrophic lateral sclerosis. *Nature* 362:59–62.
10. Lindberg MJ, Byström R, Boknäs N, Andersen PM, Oliveberg M (2005) Systematically perturbed folding patterns of amyotrophic lateral sclerosis (ALS)-associated SOD1 mutants. *Proc Natl Acad Sci USA* 102:9754–9759.
11. Valentine JS, Doucette PA, Zittin Potter S (2005) Copper-zinc superoxide dismutase and amyotrophic lateral sclerosis. *Annu Rev Biochem* 74:563–593.
12. Hart PJ (2006) Pathogenic superoxide dismutase structure, folding, aggregation and turnover. *Curr Opin Chem Biol* 10:131–138.
13. Gurney ME, et al. (1994) Motor neuron degeneration in mice that express a human Cu,Zn superoxide dismutase mutation. *Science* 264:1772–1775.
14. Bruijn LI, Miller TM, Cleveland DW (2004) Unraveling the mechanisms involved in motor neuron degeneration in ALS. *Annu Rev Neurosci* 27:723–749.
15. Münch C, O'Brien J, Bertolotti A (2011) Prion-like propagation of mutant superoxide dismutase-1 misfolding in neuronal cells. *Proc Natl Acad Sci USA* 108:3548–3553.
16. Grad LI, et al. (2014) Intercellular propagated misfolding of wild-type Cu/Zn superoxide dismutase occurs via exosome-dependent and -independent mechanisms. *Proc Natl Acad Sci USA* 111:3620–3625.
17. Ayers JI, et al. (2014) Experimental transmissibility of mutant SOD1 motor neuron disease. *Acta Neuropathol* 128:791–803.
18. Ayers JI, Fromholt SE, O'Neal VM, Diamond JH, Borchelt DR (2016) Prion-like propagation of mutant SOD1 misfolding and motor neuron disease spread along neuroanatomical pathways. *Acta Neuropathol* 131:103–114.
19. Bidhendi EE, et al. (2016) Two superoxide dismutase prion strains transmit amyotrophic lateral sclerosis-like disease. *J Clin Invest* 126:2249–2253.
20. Wang J, et al. (2009) Progressive aggregation despite chaperone associations of a mutant SOD1-YFP in transgenic mice that develop ALS. *Proc Natl Acad Sci USA* 106(5):1392–1397.
21. Farr GW, Ying Z, Fenton WA, Horwich AL (2011) Hydrogen-deuterium exchange in vivo to measure turnover of an ALS-associated mutant SOD1 protein in spinal cord of mice. *Protein Sci* 20:1692–1696.
22. Brown EH, King RC (1964) Studies on the events resulting in the formation of an egg chamber in *Drosophila melanogaster*. *Growth* 28:41–81.
23. Urushitani M, Ezzi SA, Julien J-P (2007) Therapeutic effects of immunization with mutant superoxide dismutase in mice models of amyotrophic lateral sclerosis. *Proc Natl Acad Sci USA* 104:2495–2500.
24. Caroni P (1997) Overexpression of growth-associated proteins in the neurons of adult transgenic mice. *J Neurosci Methods* 71:3–9.

25. Towne C, Setola V, Schneider BL, Aebischer P (2011) Neuroprotection by gene therapy targeting mutant SOD1 in individual pools of motor neurons does not translate into therapeutic benefit in fALS mice. *Mol Ther* 19:274–283.

26. Singh MS, et al. (2016) Transplanted photoreceptor precursors transfer proteins to host photoreceptors by a mechanism of cytoplasmic fusion. *Nat Commun* 7, 10.1038/ncomms13537.

27. Santos-Ferreira T, et al. (2016) Retinal transplantation of photoreceptors results in donor-host cytoplasmic exchange. *Nat Commun* 7, 10.1038/ncomms13028.

28. Pearson RA, et al. (2016) Donor and host photoreceptors engage in material transfer following transplantation of post-mitotic photoreceptor precursors. *Nat Commun* 7, 10.1038/ncomms13029.

29. Lee Y, et al. (2012) Oligodendroglia metabolically support axons and contribute to neurodegeneration. *Nature* 487:443–448.

30. Pringle NP, Richardson WD (1993) A singularity of PDGF alpha-receptor expression in the dorsoventral axis of the neural tube may define the origin of the oligodendrocyte lineage. *Development* 117:525–533.

31. Kessaris N, et al. (2006) Competing waves of oligodendrocytes in the forebrain and postnatal elimination of an embryonic lineage. *Nat Neurosci* 9:173–179.

32. Lu QR, et al. (2002) Common developmental requirement for *Olig* function indicates a motor neuron/oligodendrocyte connection. *Cell* 109:75–86.

33. Zhou Q, Anderson DJ (2002) The bHLH transcription factors OLIG2 and OLIG1 couple neuronal and glial subtype specification. *Cell* 109:61–73.

34. Kang SH, et al. (2013) Degeneration and impaired regeneration of gray matter oligodendrocytes in amyotrophic lateral sclerosis. *Nat Neurosci* 16:571–579.

35. Philips T, et al. (2013) Oligodendrocyte dysfunction in the pathogenesis of amyotrophic lateral sclerosis. *Brain* 136:471–482.

36. Ferraiuolo L, et al. (2016) Oligodendrocytes contribute to motor neuron death in ALS via SOD1-dependent mechanism. *Proc Natl Acad Sci USA* 113:E6496–E6505.

37. Hadzipasic M, et al. (2014) Selective degeneration of a physiological subtype of spinal motor neuron in mice with SOD1-linked ALS. *Proc Natl Acad Sci USA* 111:16883–16888.

38. Nagy M, Fenton WA, Li D, Furtak K, Horwich AL (2016) Extended survival of misfolded G85R SOD1-linked ALS mice by transgenic expression of chaperone Hsp110. *Proc Natl Acad Sci USA* 113:5424–5428.

39. Behringer R, Gertsenstein M, Nagy KV, Nagy A (2014) Production of chimeras. *Manipulating the Mouse Embryo: A Laboratory Manual* (Cold Spring Harbor Press, Cold Spring Harbor, NY), pp 489–513.

40. Franklin KBJ, Paxinos G (2008) *The Mouse Brain in Stereotaxic Coordinates* (Academic, New York).

41. Gray JT, Zolotukhin S (2011) Design and construction of functional AAV vectors. *Methods Mol Biol* 807:25–46.